Stresses in Subgrade under Rigid Pavement

GERALD PICKETT, *Professor of Mechanics*, and
DANIEL K. Y. AI, *Graduate Student*,
University of Wisconsin

SIMPLIFIED expressions for the theoretical stresses in the subgrade under a pavement are obtained. The simplification results from the substitution of an arbitrary combination of two solutions based upon plate theory for the usual rigorous solution of a two-layered system. The range of application of the substitute solution is greatly extended by arbitrary choice in each component solution of the factor which expresses the effect of the Poisson's ratios of pavement and subgrade on the radius of relative stiffness.

Use of the simplified expressions is facilitated by the inclusion of tables from which the stresses for given conditions may be obtained by interpolation.

● THE question of subgrade stresses has been considered by Burmister and others in their studies of two- and three-layer systems (*1*, *2*, *3*). In general the expressions they obtain for stresses are involved and require considerable computational work to evaluate. Moreover, the elastic constants of the pavement and the subgrade enter in in such a way that separate calculations are required for each different ratio of these properties. The purpose of this paper is to obtain, by a few simplifying assumptions and semiempirical methods, much-simpler expressions for subgrade stresses under rigid-type pavements such as cement concrete.

The primary simplification of the theory used by Burmister will be to use the theory of thin plates for the concrete pavement. This is the usual assumption when the study is confined to the bending of the concrete pavement (*4*, *5*). However, this simplification without modification would result in appreciable error in cases of practical importance, since it does not take into account the effects of shear in the pavement on deflection and does not properly take into account horizontal shear at the interface between subgrade and pavement. In the analysis given here, a modification is introduced which, in effect, takes these other factors into account, with the result that the simplified theory, as modified, gives results that are in agreement with the more-rigorous theory used by Burmister over a wide range of conditions.

In both cases—the Burmister theory and the simplified theory—an assumption has to be made in regard to the conditions at the interface between the pavement and the subgrade. Burmister considered two possibilities: (1) there is no friction at the interface or (2) there is continuity of displacements and boundary stresses at the interface. There are also two possibilities when plate theory is used for the pavement: (1) there is no friction at the interface and (2) no horizontal displacement is permitted at the interface.

It is of interest that the two assumptions for plate theory lead to identical expressions for the bending of the pavement slab, with the exception that the radius of relative stiffness is slightly different in the two cases. This is shown by the following equations:

$$l = h\beta[E_1/E_2]^{1/3} \qquad (1)$$

where

h is pavement thickness
E_1 is Young's modulus for pavement
E_2 is Young's modulus for subgrade
β is a factor that depends on the Poisson's ratios and is different for the two cases.

For no friction at interface:

$$\beta = [(1 - \mu^2)/6(1 - \nu^2)]^{1/3} \qquad (2)$$

For no horizontal displacement at interface:

$$\beta = [(3 - 4\mu)(1 + \mu)/24(1 - \mu)(1 - \nu^2)]^{1/3} \qquad (3)$$

where

μ is Poisson's ratio for subgrade
ν is Poisson's ratio for pavement.

The first modification introduced is to use an arbitrary value for β in either solution instead of that given by Equations 2 or 3. The second modification is to combine both solutions in an arbitrary way. If in the Burmister theory the assumption of no friction at the interface is made, then only the one plate theory solution, that of no friction, is needed. If in the Burmister theory continuity at the interface is assumed, then g parts of the one solution based on plate theory is added to $(1 - g)$ parts of the other solution based on plate theory. The basis for determining g is to make the shear at the interface approximately the same as that given by the Burmister theory. The basis for determining β in each solution is to make the shapes of the two curves obtained from plotting shear stress and normal stress at the interface versus radial distance from the load agree best with the Burmister theory. If these interface stresses are approximately the same as in the Burmister theory, then all subgrade stresses at all points will be in good agreement with his theory.

SUBGRADE STRESSES BASED ON PLATE THEORY FOR THE PAVEMENT

The pavement is assumed to be governed by the well known plate equation

$$\frac{E_1 h^3}{12(1 - \nu^2)} \nabla^2 \nabla^2 w = q - p \qquad (4)$$

where q is the loading on top and p is the reactive pressure between pavement and subgrade. The subgrade is assumed to be governed by the Love strain function ϕ which must satisfy Equation 6.

$$\nabla^2 \nabla^2 \phi = 0 \qquad (5)$$

Subgrade stresses are found from solutions for ϕ by means of the relations

$$\sigma_z = \frac{\partial}{\partial z}\left[(2 - \mu)\nabla^2\phi - \frac{\partial^2\phi}{\partial z^2}\right] \qquad (6)$$

$$\sigma_r = \frac{\partial}{\partial z}\left[\mu\nabla^2\phi - \frac{\partial^2\phi}{\partial r^2}\right] \qquad (7)$$

$$\sigma_\theta = \frac{\partial}{\partial z}\left[\mu\nabla^2\phi - \frac{1}{r}\frac{\partial\phi}{\partial r}\right] \qquad (8)$$

$$\tau_{rz} = \frac{\partial}{\partial r}\left[(1 - \mu)\nabla^2\phi - \frac{\partial^2\phi}{\partial z^2}\right] \qquad (9)$$

The use of Love's strain function necessitates the assumption that all stresses are independent of the cylindrical coördinate θ. This assumption is made.

If the load on the pavement is uniformly distributed over a circular area of radius a, then ϕ becomes:

For no friction at interface:

$$\phi = -qal^2 \cdot \int_0^\infty \frac{(2\mu + \alpha\zeta)J_0(\alpha\rho)J_1\left(\frac{\alpha a}{l}\right)e^{-\alpha\zeta}\,d\alpha}{\alpha^3(1 + \alpha^3)} \qquad (10)$$

For no horizontal displacement at interface:

$$\phi = -\frac{qal^2}{2(1 - \mu)} \cdot \int_0^\infty \frac{(1 + \alpha\zeta)J_0(\alpha\rho)J_1\left(\frac{\alpha a}{l}\right)e^{-\alpha\zeta}\,d\alpha}{\alpha^3(1 + \alpha^3)} \qquad (11)$$

where $\rho = r/l$ and $\zeta = z/l$.

After substituting the appropriate ϕ into Equations 6 to 9 and expanding $J_1\left(\frac{\alpha a}{l}\right)$ into a power series, the following equations are obtained:

For no friction at the interface:

$$\sigma_z = -\frac{qa}{l}\sum_{k=0}^{\infty} A_k\left(\frac{a}{l}\right)[F_{0,2k+1} + \zeta F_{0,2k+2}] \qquad (12)$$

$$\sigma_r = -q\frac{a}{l}\sum_{k=0}^{\infty} A_k\left(\frac{a}{l}\right)[F_{0,2k+1} - \zeta F_{0,2k+2} - (1 - 2\mu)F_{1,2k} + \zeta F_{1,2k+1}] \qquad (13)$$

$$\sigma_\theta = -q\frac{a}{l}\sum_{k=0}^{\infty} A_k\left(\frac{a}{l}\right) \cdot [2\mu F_{0,2k+1} + (1 - 2\mu)F_{1,2k} - \zeta F_{1,2k+1}] \qquad (14)$$

$$\tau_{rz} = -q\frac{a\zeta\rho}{l}\sum_{k=0}^{\infty} A_k\left(\frac{a}{l}\right)F_{1,2k+2} \qquad (15)$$

For no horizontal displacement at interface:

$$\sigma_z = -\frac{qa}{2(1-\mu)l}\sum_{k=0}^{\infty} A_k\left(\frac{a}{l}\right) \cdot[2(1-\mu)F_{0,2k+1} + \zeta F_{0,2k+2}] \quad (16)$$

$$\sigma_r = -\frac{qa}{2(1-\mu)l}\sum_{k=0}^{\infty} A_k\left(\frac{a}{l}\right) \cdot[2\mu F_{0,2k+1} - \zeta F_{0,2k+2} + \zeta F_{1,2k+1}] \quad (17)$$

$$\sigma_\theta = -\frac{qa}{2(1-\mu)l}\sum_{k=0}^{\infty} A_k\left(\frac{a}{l}\right) \cdot[2\mu F_{0,2k+1} - \zeta F_{1,2k+1}] \quad (18)$$

$$\tau_{rz} = -\frac{qal}{2(1-\mu)l}\sum_{k=0}^{\infty} A_k\left(\frac{a}{l}\right) \cdot[(1-2\mu)F_{1,2k+1} + \zeta F_{1,2k+2}] \quad (19)$$

where

$$A_k\left(\frac{a}{l}\right) = \left(\frac{a}{2l}\right)^{2k+1} \Big/ k\,!\,(k+1)! \quad (20)$$

$$F_{0n} = \int_0^\infty \frac{J_0(\alpha\rho)e^{-\alpha\zeta}}{1+\alpha^3}\alpha^n\, d\alpha \quad (21)$$

$$F_{1n} = \frac{1}{\rho}\int_0^\infty \frac{J_1(\alpha\rho)e^{-\alpha\zeta}}{1+\alpha^3}\alpha^n\, d\alpha \quad (22)$$

The particular expressions for ϕ in Equations 10 and 11 were chosen not only to satisfy Equation 5 but the plate equation, Equation 4. For this purpose w is taken as being the deflection of the subgrade at $z = 0$, or

$$w = \frac{1+\mu}{E_2}\left[2(1-\mu)\nabla^2\phi - \frac{\partial^2\phi}{\partial z^2}\right]_{z=0} \quad (23)$$

The pressure p is the negative of σ_z at $z = 0$, and the load q is q for $r \leq a$ and zero for $r > a$. The appropriate expression for β, Equations 2 and 3, is also required if Equation 4 is to be satisfied.

The requirement that τ_{rz} be zero at $z = 0$ in the first solution is obviously met by Equation 15. The requirement of no horizontal displacement at the interface is met for the second solution, since for it

$$-\frac{(1+\mu)}{E^2}\frac{\partial^2\phi}{\gamma r\,\partial z}\bigg|_{z=0} = 0 \quad (24)$$

All the expressions for stresses are convergent and rapidly so if a/l is not large. If a/l is zero, that is, the load is concentrated at a point, then only the first term in the summations remains. Other simplifications result if either ρ or ζ is zero, and still further simplifications if two of the three parameters a/l, ρ, ζ are zero.

For numerical computations tables of the F functions are desired. The function F_{0n} may be reduced to one of the three functions F_{00}, F_{01}, F_{02}, and F_{1n} may be reduced to one of F_{10}, F_{11}, F_{12} by repeated application of the following formulas:

$$F_{0,m+3} = -F_{0m} + (-1)^m\frac{\partial^m}{\gamma\zeta^m}[\rho^2+\zeta^2]^{-1/2} \quad (25)$$

$$F_{1,m+3} = -F_{1m} + \frac{(-1)^{m-1}}{\rho^2}\frac{\partial^m}{\partial\zeta^m}\left[\frac{\zeta}{(\rho^2+\zeta^2)^{3/2}}\right] \quad (26)$$

Numerical values for the six basic F functions for a limited range of ρ and ζ are given in Tables 1 to 6. Their use is illustrated by the following example:

Example: In Equation 12 let $a/l = 0.5$, $\rho = 1.0$, $\zeta = 1.2$. Then

$$\sigma_z = -0.5q[.25F_{01} + .30F_{02} + .0078125F_{03} + .009375F_{04} + .000081F_{05} + \cdots] \quad (27)$$

TABLE 1

$$F_{00} = \int_0^\infty \frac{J_0(\alpha\rho)\,e^{-\alpha\zeta}}{1+\alpha^3}\,d\alpha$$

	0.0	0.2	0.4	0.6	0.8	1.0	1.2	1.4	1.6	1.8	2.0
0.0	1.20920	1.18192	1.12747	1.06066	0.98853	0.91526	0.84347	0.77482	0.71029	0.65042	0.59543
0.2	1.01934	1.00756	.97582	.93139	.87968	.82449	.76841	.71284	.66015	.60996	.56304
0.4	.88446	.87714	.85644	.82552	.78767	.74566	.70164	.65690	.61357	.57150	.53154
0.6	.78025	.77521	.76068	.73825	.70988	.67746	.64262	.60645	.57072	.53545	.50145
0.8	.69675	.69309	.68239	.66557	.64381	.61842	.59059	.56116	.53160	.50198	.47303
1.0	.62831	.62549	.61734	.60433	.58736	.56719	.54472	.52062	.49603	.47108	.44639
1.2	.57104	.56889	.56253	.55232	.53879	.52254	.50423	.48433	.46378	.44268	.42157
1.4	.52259	.52088	.51581	.50763	.49670	.48346	.46838	.45184	.43456	.41664	.39854
1.6	.48106	.47968	.47558	.46893	.45999	.44908	.43655	.42269	.40808	.39280	.37722
1.8	.44513	.44399	.44063	.43516	.42776	.41868	.40819	.39650	.38406	.37097	.35751
2.0	.41376	.41282	.41003	.40548	.39930	.39168	.38282	.37289	.36225	.35098	.33931

TABLE 2

$$F_{01} = \int_0^\infty \frac{J_0(\alpha\rho)\epsilon^{-\alpha\zeta}}{1+\alpha^3}\,\alpha d\alpha$$

	0.0	0.2	0.4	0.6	0.8	1.0	1.2	1.4	1.6	1.8	2.0
0.0	1.20920	1.02121	0.85655	0.71370	0.59078	0.48581	0.39678	0.32177	0.25896	0.20669	0.16341
0.2	.77649	.74495	.66933	.58364	.50010	.42308	.35426	.29378	.24193	.19799	.16044
0.4	.58693	.57147	.53176	.47912	.42233	.33637	.31389	.26578	.22365	.18646	.15424
0.6	.46330	.45466	.43090	.39695	.35772	.31690	.27694	.23902	.20483	.17384	.14642
0.8	.37621	.37080	.35541	.33245	.30468	.27459	.24406	.21419	.18654	.16089	.13770
1.0	.31176	.30811	.29757	.28141	.26127	.23876	.21527	.19168	.16932	.14814	.12863
1.2	.26242	.25983	.25230	.24056	.22562	.20853	.19028	.17156	.15345	.13597	.11958
1.4	.22369	.22179	.21624	.20749	.19617	.18301	.16869	.15374	.13902	.12457	.11081
1.6	.19268	.19127	.18708	.18041	.17169	.16141	.15007	.13804	.12601	.11404	.10248
1.8	.16750	.16641	.16318	.15802	.15119	.14306	.13398	.12424	.11436	.10441	.09468
2.0	.14676	.14591	.14338	.13931	.13390	.12740	.12006	.11211	.10395	.09565	.08743

TABLE 3

$$F_{02} = \int_0^\infty \frac{J_0(\alpha\rho)\epsilon^{-\alpha\zeta}}{1+\alpha^3}\,\alpha^2 d\alpha$$

ζ \ ρ	0.0	0.2	0.4	0.6	0.8	1.0	1.2	1.4	1.6	1.8	2.0
0.0	∞	1.73660	1.07396	0.71393	0.48320	0.32516	0.21378	0.13429	0.07747	0.03713	0.00890
0.2	1.26737	1.07326	.80261	.58537	.42196	.30119	.20784	.14222	.08649	.05428	.02453
0.4	.74939	.69888	.58504	.46293	.35492	.26572	.19420	.13758	.09402	.06098	.03584
0.6	.51099	.48893	.43300	.36281	.29254	.22906	.17476	.12945	.09338	.06454	.04186
0.8	.37066	.35919	.32821	.28574	.23949	.19466	.15404	.11851	.08909	.06463	.04484
1.0	.27982	.27312	.25440	.22738	.19624	.16440	.13415	.10655	.08286	.06251	.04555
1.2	.21729	.21305	.20102	.18307	.16157	.13867	.11607	.09472	.07579	.05904	.04471
1.4	.17238	.16956	.16146	.14911	.13388	.11718	.10018	.08363	.06855	.05486	.04285
1.6	.13911	.13717	.13151	.12275	.11173	.09936	.08645	.07358	.06156	.05040	.04039
1.8	.11387	.11248	.10841	.10205	.09392	.08462	.07472	.06465	.05505	.04596	.03764
2.0	.09433	.09331	.09032	.08560	.07949	.07241	.06474	.05681	.04911	.04170	.03479

TABLE 4

$$F_{10} = \frac{1}{\rho}\int_0^\infty \frac{J_1(\alpha\rho)\epsilon^{-\alpha\zeta}}{1+\alpha^3}\,d\alpha$$

ζ \ ρ	0.0	0.2	0.4	0.6	0.8	1.0	1.2	1.4	1.6	1.8	2.0
0.0	0.60460	0.54094	0.48318	0.43103	0.38415	0.34214	0.30462	0.27119	0.24147	0.21510	0.19173
0.2	.38825	.38075	.35946	.33303	.30533	.27811	.25225	.22814	.20595	.18331	.16736
0.4	.29346	.28961	.27903	.26410	.24688	.22876	.21065	.19310	.17643	.16084	.14640
0.6	.23165	.22948	.22332	.21409	.20282	.19039	.17746	.16453	.15191	.13984	.12843
0.8	.18810	.18675	.18281	.17672	.16901	.16022	.15081	.14114	.13150	.12208	.11303
1.0	.15588	.15497	.15228	.14806	.14259	.13621	.12922	.12190	.11445	.10705	.09983
1.2	.13121	.13056	.12865	.12561	.12161	.11687	.11159	.10596	.10015	.09429	.08849
1.4	.11184	.11137	.10997	.10771	.10472	.10113	.09707	.09269	.08810	.08342	.07874
1.6	.09634	.09599	.09493	.09323	.09094	.08817	.08500	.08155	.07790	.07413	.07032
1.8	.08375	.08348	.08267	.08135	.07957	.07740	.07490	.07215	.06921	.06615	.06303
2.0	.07338	.07317	.07253	.07150	.07009	.06837	.06637	.06416	.06178	.05927	.05670

TABLE 5

$$F_{11} = \frac{1}{\rho}\int_0^\infty \frac{J_1(\alpha\rho)\epsilon^{-\alpha\zeta}}{1+\alpha^3}\,\alpha d\alpha$$

ζ \ ρ	0.0	0.2	0.4	0.6	0.8	1.0	1.2	1.4	1.6	1.8	2.0
0.0	∞	1.11554	0.77686	0.58619	0.45779	0.36435	0.29345	0.23826	0.19456	0.15958	0.13134
0.2	0.63369	.57607	.48935	.40682	.33731	.27998	.23276	.19389	.16169	.13499	.11299
0.4	.37470	.36192	.32974	.29079	.25213	.21664	.18520	.15786	.13429	.11412	.09696
0.6	.25550	.24989	.23491	.21441	.19184	.16938	.14823	.12983	.11166	.09642	.08309
0.8	.18533	.18245	.17435	.16253	.13414	.13401	.11954	.10580	.09309	.08155	.07121
1.0	.13991	.13823	.13340	.12609	.11714	.10731	.09723	.08733	.07791	.06913	.06109
1.2	.10865	.10759	.10450	.09973	.09373	.08694	.07977	.07254	.06549	.05878	.05251
1.4	.08619	.08549	.08342	.08018	.07601	.07120	.06601	.06066	.05533	.05017	.04525
1.6	.06956	.06907	.06763	.06535	.06238	.05890	.05507	.05105	.04699	.04298	.03911
1.8	.05694	.05659	.05556	.05391	.05174	.04917	.04630	.04324	.04011	.03698	.03391
2.0	.04717	.04691	.04616	.04494	.04333	.04139	.03824	.03686	.03442	.03195	.02950

TABLE 6

$$F_{12} = \frac{1}{\rho}\int_0^\infty \frac{J_1(\alpha\rho)e^{-\alpha\zeta}}{1+\alpha^3}\,\alpha^2 d\alpha$$

ζ \ ρ	0.0	0.2	0.4	0.6	0.8	1.0	1.2	1.4	1.6	1.8	2.0
0.0	∞	4.40284	1.91830	1.10465	0.71006	0.48335	0.34040	0.24495	0.17877	0.13169	0.097575
0.2	1.99033	1.54713	1.04687	.71494	.50443	.36493	.26849	.20009	.15030	.11265	.085691
0.4	.80777	.73999	.60045	.46509	.35606	.27261	.20928	.16130	.12447	.096189	.074666
0.6	.44321	.42254	.37179	.31100	.25330	.20352	.16238	.12910	.10240	.081104	.064203
0.8	.27662	.26805	.24542	.21514	.18311	.15288	.12607	.10311	.083841	.067789	.054798
1.0	.18584	.18166	.17008	.15358	.13487	.11602	.098326	.082420	.068525	.056616	.046543
1.2	.13115	.12882	.12231	.11267	.10121	.089100	.077215	.066099	.056041	.047150	.039422
1.4	.095848	.094472	.090546	.084585	.077267	.069263	.061128	.053267	.045938	.039281	.033352
1.6	.071970	.071103	.068610	.064758	.059917	.054482	.048807	.043175	.037789	.032780	.028221
1.8	.055213	.054646	.052997	.050415	.047116	.043336	.039303	.035213	.031218	.027426	.023906
2.0	.043120	.042732	.041604	.039822	.037514	.034828	.031914	.028904	.025911	.023019	.020290

By Equation 25

$$F_{03} = -F_{00} + [1 + 1.44]^{-1/2}$$

$$F_{04} = -F_{01} + 1.2[1 + 1.44]^{-3/2}$$

$$F_{05} = -F_{02} + (2 \times 1.44 - 1)[1 + 1.44]^{-5/2}$$

From the tables

$$F_{00} = 0.52254$$

$$F_{01} = 0.20853$$

$$F_{02} = 0.13867$$

Therefore

$$F_{03} = -.52254 + .64018 = .11764$$

$$F_{04} = -.20853 + .31484 = .10631$$

$$F_{05} = -.13867 + .20215 = .06348$$

$$\sigma_z = -0.5[.05213 + .04160 + .00092 + .00100 + .00001]q$$

$$\sigma_z = -0.04783\,q$$

In general two-dimensional interpolation is necessary when using the tables, since the F functions depend on two variables, ζ and ρ. In some cases interpolation within the limited tables given here may not give the accuracy desired. Fortunately there are three ranges of the variables ζ and ρ for which satisfactory formulas are available. These are as follows:

For ζ large and equal to or greater than ρ.

$$F_{mn} = \sum_{k=0}^{\infty}\sum_{j=0}^{\infty} \frac{(-1)^{j+k}(m+n+3j+2k)!\left(\frac{\rho}{2\zeta}\right)^{2k}}{2^m k!(m+k)!\zeta^{m+n+3j+1}} \quad (28)$$

For ρ small and less than or equal to ζ.

$$F_{mn} = \sum_{k=0}^{\infty} \frac{(-1)^k \rho^{2k} f_{2k+m+n}(\zeta)}{2^{m+2k}k!(m+k)!} \quad (29)$$

For ζ small and less than or equal to ρ.

$$F_{0n} = \sum_{k=0}^{\infty} \frac{(-1)^k \zeta^k}{k!} U_{n+k}(\rho) \quad (30)$$

$$F_{1n} = \frac{1}{\rho}\sum_{k=0}^{\infty} \frac{(-1)^k \zeta^k}{k!} V_{n+k}(\rho) \quad (31)$$

where

$$f_n(\zeta) = \int_0^\infty \frac{\alpha^n e^{-\alpha\zeta}}{1+\alpha^3}\,d\alpha \quad (32)$$

$$U_n(\rho) = \int_0^\infty \frac{\alpha^n J_0(\alpha\rho)\,d\alpha}{1+\alpha^3} \quad (33)$$

$$V_n(\rho) = \int_0^\infty \frac{\alpha^n J_1(\alpha\rho)\,d\alpha}{1+\alpha^3} \quad (34)$$

The functions $f_0(\zeta)$, $f_1(\zeta)$, and $f_2(\zeta)$ were investigated and tables prepared in work done for the Army Corps of Engineers, soon to be published. The remaining f's may be expressed in terms of these three by the reduction formula

$$f_{n+3}(\zeta) = -f_n(\zeta) + \frac{n!}{\zeta^{n+1}} \quad (35)$$

The six functions U_0, U_1, U_2, V_{-1}, V_0, V_1 are given in tabular form in Table 1, page 61 of reference 5. The remainder of these may be obtained by the reduction formulas

$$U_{n+3}(\rho) = -U_n(\rho) + \begin{cases} 0 \text{ if } n \text{ is odd} \\ (-1)^{n/2}\dfrac{[1\cdot 3\cdot 5\cdots(n-1)]}{\rho^{n+1}} \end{cases} \text{ if } n \text{ is even.}$$

$$V_{n+3}(\rho) = -V_n(\rho) + \delta_n$$

where

$$\delta_{-1} = 1$$

$$\delta_0 = \frac{1}{\rho}$$

$\delta_n = 0$ if $n > 0$ and even

$$\delta_n = (-1)^{(n-1)/2} \frac{[1 \cdot 3 \cdot 5 \cdots n]^2}{n\rho^{n+1}}$$

if $n > 0$ and odd.

Use was made of these special formulas and of the tables of f, U, and V in preparing the tables for the F functions. However, most of the tabulated values were obtained by numerical integration using IBM equipment.

MODIFICATION OF THE PLATE-THEORY SOLUTIONS

The solutions based on thin plate theory for the pavement may be modified by using an arbitrary value for β in each solution instead of those given by Equations 2 and 3. By using a reduced value the effects of deflection due to shear and of other factors neglected in the derivation of Equation 4 are accounted for to some extent. By taking g parts of one solution and $(1 - g)$ parts of the other solution, three adjustable parameters, two β's and g, become available for the modified plate theory solution. The determination of these three parameters or their equivalents so as to bring the modified plate theory solution into good agreement with the Burmister theory will now be considered.

Certain special solutions based upon the Burmister theory are necessary to provide a basis for selecting the adjustable parameters. The solutions used will be those for interface stresses caused by a concentrated load. The interface stresses are a normal stress σ_z and a shear stress τ_{rz}. They are given by:

$$\sigma_z = -\frac{P}{2\pi h^2} B_\sigma \tag{36}$$

$$\tau_{rz} = -\frac{P}{2\pi h^2} B_\tau \tag{37}$$

where

$$B_\sigma = \int_0^\infty \frac{[1 - 0.5(L + K) + (1 - K)\alpha]e^{-\alpha} + [KL - 0.5(L+K) + (1-L)K\alpha]e^{-3\alpha}}{1 - (L + K + 4K\alpha^2)e^{-2\alpha} + KLe^{-4\alpha}} \cdot J_0\left(\frac{\alpha r}{h}\right) \alpha d\alpha$$

$$B_\tau = \int_0^\infty \frac{[0.5(L-K) + (1-K)\alpha]e^{-\alpha} + [0.5(K-L) - (1-L)K\alpha]e^{-3\alpha}}{1 - (L + K + 4K\alpha^2)e^{-2\alpha} + KLe^{-4\alpha}} \cdot J_1\left(\frac{\alpha r}{h}\right) \alpha \, d\alpha$$

$$K = \frac{1 - n}{1 + n(3 - 4\nu)},$$

$$L = \frac{3 - 4\mu - n(3 - 4\nu)}{3 - 4\mu + n}, \qquad n = \frac{E_2(1 + \nu)}{E_1(1 + \mu)}$$

Values of B_σ and B_τ for six different combinations of K and L and for various values of r/h are given in Tables 7 and 8, respec-

TABLE 7
B_σ

r/h	K = .94 L = .94	K = .94 L = .96	K = .96 L = .96	K = .96 L = .98	K = .98 L = .98	K = .98 L = .99
0	0.448408	0.420846	0.339422	0.306315	0.210983	0.178913
1.0	.245987	.228775	.201425	.179158	.139837	.121803
2.0	.133096	.125157	.119313	.107523	.0936337	.0835560
5.0	.0187949	.0197420	.0231457	.0237175	.0274422	.0267515

TABLE 8
B_τ

r/h	K = .94 L = .94	K = .94 L = .96	K = .96 L = .96	K = .96 L = .98	K = .98 L = .98	K = .98 L = .99
0	0	0	0	0	0	0
0.2	0.041938	0.046070	0.028508	0.033022	0.014648	0.017209
0.4	.067421	.075015	.046020	.054379	.023785	.028572
0.6	.074729	.084888	.051385	.062673	.026827	.033374
0.8	.071593	.083528	.049732	.063153	.026331	.034234
1.0	.064965	.078117	.046006	.060674	.024609	.033570
1.5	.049660	.064410	.036186	.053548	.020450	.031241
2.0	.038658	.053792	.029220	.047607	.017357	.029212
5.0	.007407	.016727	.007253	.020779	.006116	.016915

tively. The variations in K and L correspond roughly to a variation in E_1/E_2 from 50 to 150 and to reasonable variations in μ and ν. The tables were obtained by numerical integration using IBM equipment.

The corresponding solutions based on plate theory are:

For no friction at interface[1]

$$\sigma_z = -\frac{P}{2\pi h^2}\left(\frac{h}{l_1}\right)^2 U_1(r/l_1) \tag{38}$$

$$\tau_{rz} = 0 \tag{39}$$

For no horizontal displacement at interface

$$\sigma_z = -\frac{P}{2\pi h^2}\left(\frac{h}{l_2}\right)^2 U_1(r/l_2) \tag{40}$$

$$\tau_{rz} = -\frac{P}{2\pi h^2}\frac{(1-2\mu)}{2(1-\mu)}\left(\frac{h}{l_2}\right)^2 V_1(r/l_2) \tag{41}$$

The problem then becomes one of selecting the adjustable parameters (l_1/h), (l_2/h), and g so as to satisfy the following relations as well as possible.

$$g(h/l_1)^2 U_1\left(\frac{r}{l_1}\right) + (1-g)(h/l_2)^2 U_1(r/l_2) = B_\sigma \tag{42}$$

$$(1-g)\frac{1-2\mu}{2(1-\mu)}\left(\frac{h}{l_2}\right)^2 V_1(r/l_2) = B_\tau \tag{43}$$

Since B_σ and B_τ are functions of K and L, it is obvious from Equations 42 and 43 that the adjustable parameters depend on μ, K, and L. Eventually it is desirable to use μ, ν, and E_1/E_2 instead of μ, K, and L for the elastic properties and, because of less variation, it is desirable to use β_1 and β_2 instead of (l_1/h) and (l_2/h) for adjustable parameters. Finally then it is desirable to have tables or charts from which β_1, β_2, and g may be readily determined from given values of μ, ν, and E_1/E_2. The preparation of such tables is beyond the scope of this paper. However, the determination of these parameters from available tables will now be explained.

An understanding of the functional relations involved and of the adjustments necessary are provided by Figure 1. The upper curve of Figure 1 is a plot of $(h/l)^2 U_1(r/l)$ for $(l/h) = 1.643$ versus r/h. The lower curve is a plot of 0.496 $(h/l)^2 V_1(r/l)$, also for $(l/h) = 1.643$. The plotted points near the upper curve are values of B_σ from Table 7 and the plotted points near the lower curve are values of B_τ from Table 8 for $K = 0.94$, $L = 0.94$. The value of 1.643 was selected to make the upper curve coincide with B_σ at $r = 0$. The value of 0.496 makes the peak value of the lower curve about 0.9 as much as the maximum B_τ. This selection was entirely arbitrary.

The closeness of agreement between the upper curve of Figure 1 and the plotted values of B_σ indicates that either plate solution is satisfactory as far as the interface stress σ_z is concerned. The agreement would be still better if (l/h) were selected to make the curve agree with B_σ at $r = 0.5h$. All this has been accomplished by the use of only one parameter, l/h. By combining both plate solutions and using a different (l/h) in each, as indicated by Equation 42, excellent agreement could be obtained.

The lower curve of Figure 1 and the plotted values of B_τ are not in good agreement. Fairly good agreement could be obtained by a different choice of (l/h) and the numerical factor. This would be equivalent to selecting (l_2/h) and g in Equation 43. However, the selection that would make the best agreement between the two sides of Equation 43 would in general make it impossible for the two sides of Equation 42 to agree very well even with freedom to choose (l_1/h). It appears that the best compromise is to give primary consideration to Equation 42 and then obtain the best agreement between the two sides of Equation 43 that can be obtained without appreciably affecting Equation 42. The fact that the interface shear stresses are much

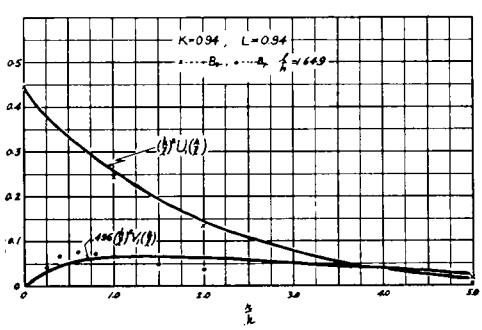

Figure 1. Comparison of plate theory with the Burmister theory, $K = 0.94$, $L = 0.94$, $l = 1.649h$.

[1] See page 61 of Kansas State College Bulletin 65 for a table of U_1 and V_1.

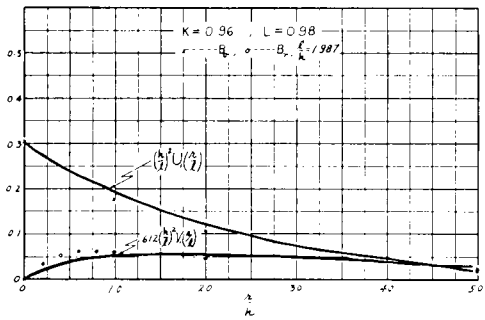

Figure 2. Comparison of plate theory with the Burmister theory, $K = 0.96$, $L = 0.98$, $l = 1.987h$.

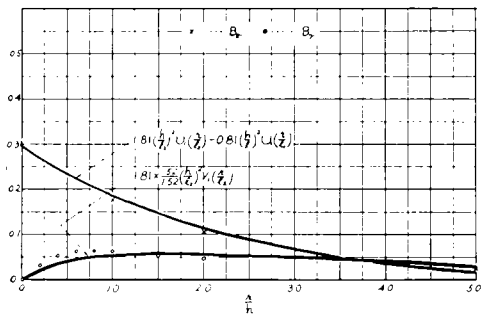

Figure 3. Comparison of plate theory with the Burmister theory, $K = 0.9599$, $L = 0.9799$, $l_1 = 1.954$, $l_2 = 2.0h$, $g = -0.81$.

smaller than the interface normal stresses is additional reason for allowing greater error in the shear stresses.

Results similar to those shown in Figure 1 were obtained for all combinations of K and L investigated, those for $K = 0.96$, $L = 0.98$ being shown by Figure 2. In Figure 2, as in Figure 1, the agreement of the upper curve with B_σ is obtained by the use of only one parameter, (l/h), which was selected to make the curve and B_σ agree at $r = 0$. Only one additional parameter was used in constructing the lower curve. Better agreement with both B_σ and B_τ can be obtained by the use of three parameters. This will be illustrated by an example.

Given $h = 8$ in., $\mu = 0.24$, $\nu = 0.20$, $E_1 = 3 \times 10^6$ psi., $E_2 = 40{,}000$ psi. From this information, $K = 0.9599$, $L = 0.9799$. By interpolation from Table 7, B_σ equals 0.236 at $r = 0.5h$. From Table 8 it appears that maximum B_τ is about 0.0632 and occurs at $r = 0.7h$. A good indication of what to use for (l_2/h) is given by the relation

$$(h/l_2)^2 U_1\left(\frac{h}{2l_2}\right) = 0.236$$

This gives $l_2/h = 2.04$. It is usually desirable to use a slightly smaller value. Try $l_2/h = 2.0$ and make the peak of the left side of Equation 43 equal to 0.9 of 0.0632.

$$(1 - g)\,\frac{.52}{1.52}\left(\frac{1}{2.0}\right)^2 0.367 = 0.9 \times .0632$$

$$(1 - g) = 1.81, \qquad g = -0.81$$

The factor 0.367 is the maximum value of V_1. Substitution in Equation 42 gives for $r = 0.5h$

$$-0.81\left(\frac{h}{l_1}\right)^2 U_1\left(\frac{h}{2l_1}\right) + 1.81\left(\tfrac{1}{2}\right)^2 U_1(0.25) = 0.236$$

or $l_1/h = 1.954$.

The upper curve of Figure 3 is a plot of the left side of Equation 42, and the lower curve is a plot of the left side of Equation 43, using the foregoing data. Also shown in Figure 3 are interpolated values of B_σ and B_τ. Although improvements could be made by using other values of the adjustable parameters, the agreement is considered satisfactory.

With (l_1/h), (l_2/h), and g determined, subgrade stresses may be found not only for the given concentrated load but also for distributed loads and for other thicknesses of pavement. These are found by means of Equations 12 to 19 and Tables 1 to 6.

CONCLUSIONS AND RECOMMENDATIONS

On the basis of the present investigation, it is concluded that theoretical stresses in the subgrade under concrete pavements can be determined with good accuracy by the modified plate theory. Since the ranges of K and L investigated correspond to a range of about 50 to 150 for E_1/E_2, the conclusions are restricted to concrete pavements.

To increase the usefulness of the method, it is recommended that tables or charts be prepared from which β_1, β_2, and g may be readily determined from given values of E_1/E_2, μ, and ν. It is recommended that the limitations of the method be determined. Perhaps it can be used for subgrades under

flexible pavements also. It is further recommended that the possibility of extending the method to more than two layers be investigated.

ACKNOWLEDGMENTS

The authors wish to express their appreciation to the University of Wisconsin and to the Wisconsin Alumni Research Foundation for salary support and to the Numerical Analysis Laboratory of the University for assistance in the numerical work.

REFERENCES

1. "The Theory of Stresses and Displacements in Layered Systems and Applications to the Design of Airport Runways," by D. M. BURMISTER, Proc. of the Twenty-third Annual Meeting of the Highway Research Board, 1943, pp. 126–44.
2. "Computation of Traffic Stresses in a Simple Road Structure," by L. Fox, D.S.I.R., Road Res. Tech. Paper No. 9, 1948.
3. "Computation of Load Stresses in a Three-layer Elastic System," by W. E. A. ACUM AND L. FOX, Geotechnique, Vol. 2, No. 4, Dec. 1951, pp. 293–300.
4. "Equilibrium of a Thin Slab on an Elastic Foundation of Finite Depth," by A. H. A. HOGG, Philosophical Magazine, and Journal of Science, April 1944, London.
5. "Deflections, Moments and Reactive Pressures for Concrete Pavements," by G. PICKETT, M. E. RAVILLE, W. C. JANES, and F. J. MCCORMICK, Bulletin No. 65, Engr. Exp. Sta., Kansas State College, Oct. 1951.
6. "The Mathematical Theory of Elasticity," 4th Ed., by A. E. H. LOVE, Cambridge Univ. Press, 1927, pp. 273–77.

Accident-Exposure Index

LEO GROSSMAN, *District Engineer*
Bureau of Public Roads

THE conventional method of portraying traffic movements at highway intersections is by means of traffic vectors. When two highways cross at grade, the vector diagram contains 16 vector crossing points which are defined as collision points. The number of these collision points is reduced to zero under two conditions only; namely, when a grade-separation structure is constructed without interchange ramps and when the grade-separation structure is constructed with a full cloverleaf or direct-connection design.

When traffic densities or economic, topographic or urban-planning considerations indicate that a partial-interchange layout is called for, it is most desirable that that traffic pattern and partial-interchange layout which will offer the greatest traffic efficiency be adopted. Using only the original traffic-vector diagram as a base, the report presents a technique whereby a numerical value or score is established for each layout under consideration. This value is termed the *accident-exposure index*. A comparison of these indices provides a direct evaluation of the traffic efficiency of the interchange. Computations are given in this report to exemplify the technique used in establishing the layout for expressway interchanges.

● COLLISIONS between two moving vehicles can occur only when both vehicles try to occupy the same space at the same time. When referring to highway accidents, such collisions can occur only under four conditions: meeting head on, rear end by overtaking, side-swiping, and crossing each others' travel path. Highway design can minimize or entirely eliminate all of the conditions under which such accidents might occur. The degree